ELSEVIER

Nuclear Instruments and Methods in Physics Research B 175–177 (2001) 350–356

NIM B
Beam Interactions with Materials & Atoms

www.elsevier.nl/locate/nimb

Anisotropic deformation of colloidal particles under MeV ion irradiation

T. van Dillen [a,*], E. Snoeks [a], W. Fukarek [c], C.M. van Kats [b], K.P. Velikov [b], A. van Blaaderen [a,b], A. Polman [a]

[a] *FOM Institute for Atomic and Molecular Physics, Kruislaan 407, NL-1098 SJ Amsterdam, The Netherlands*
[b] *Physics and Chemistry of Condensed Matter, Debye Institute, Utrecht University, Princetonplein 5, NL-3584 CC Utrecht, The Netherlands*
[c] *Research Center Rossendorf, Institute of Ion Beam Physics and Materials Research, P.O. Box 510119, D-01314 Dresden, Germany*

Abstract

Spherical silica colloids with a diameter of 1.0 μm, made by wet chemical synthesis, were irradiated with 2–16 MeV Au ions at fluences ranging from 2×10^{14} to 11×10^{14} cm^{-2}. The irradiation induces an anisotropic plastic deformation turning the spherical colloids into ellipsoidal oblates. After 16 MeV Au irradiation to a fluence of 11×10^{14} cm^{-2} a size-aspect ratio of 4.7 is achieved. The size polydispersity (~3%) remains unaffected by the irradiation. The transverse diameter increases with the electronic energy loss above a threshold value of ~0.6 keV/nm. Non-ellipsoidal colloids are observed in the case that the projected ion range is smaller than the colloid diameter. The deformation effect is also observed for micro-crystalline ZnS and amorphous TiO_2 colloids, as well as ZnS/SiO_2 core/shell particles. No deformation is observed for crystalline Al_2O_3 and Ag particles. The data provide strong support for the thermal spike model of anisotropic deformation.

PACS: 61.43.Fs; 61.80.Az; 61.80.Jh; 61.82.Ms; 62.20.Fe; 68.37.Hk; 82.70.Dd
Keywords: Anisotropic deformation; Ion irradiation; Colloid; SiO_2; Thermal spike

1. Introduction

MeV ion irradiation of amorphous materials such as metallic or silica glasses is known to cause anisotropic plastic deformation [1–5]. The result is an increase in the sample dimension perpendicular to the ion beam and a decrease in the direction parallel to the ion beam. This deformation process has been described mesoscopically by a viscoelastic model, in which it is assumed that due to the high electronic stopping power a cylindrically shaped region around the ion track is subject to transient heating (thermal spike) [6–8]. During the thermal spike shear stresses in the heated region relax, resulting in an associated shear strain that would freeze in upon cooling of the thermal spike.

* Corresponding author. Tel.: +31-20-608-1234; fax: +31-20-668-4106.
E-mail address: dillen@amolf.nl (T. van Dillen).

0168-583X/01/$ - see front matter
PII: S0168-583X(00)00611-X

Experimentally, the anisotropic deformation has been studied by observing macroscopic dimensional changes of (metallic) glass foils [1,2] or by studying the wafer curvature induced by irradiated thin films constrained on a substrate [4,5,9]. Recently, we have discovered that the deformation process also occurs in free-standing colloidal particles [10]. Spherical colloidal SiO_2 particles can be changed into ellipsoidal shaped particles (oblates) due to a biaxial expansion perpendicular to the ion beam and a concomitant contraction along the ion beam. Colloidal particles with variable shape can find many applications in studies of self-assembly and phase behavior [10,11] and, except ion irradiation, no other methods exist that can produce ellipsoidal inorganic colloids that are monodisperse in size and shape.

In this paper, we study the dependence of the deformation of spherical silica particles on the Au ion energy in the range 2–16 MeV. The data are consistent with the thermal spike model. In addition, we study the deformation of micro-crystalline ZnS and amorphous TiO_2 colloids, ZnS/SiO_2 core/shell particles, as well as single-crystalline Al_2O_3 and micro-crystalline Ag particles.

2. Experimental

Colloidal silica spheres were made in a solution containing tetra-ethoxysilane, ammonia and ethanol [12]. A drop of the colloidal dispersion was dried on a Si(1 0 0) substrate which had previously been cleaned in a KOH-ethanol solution. Next, the particles were irradiated with Au ions using the 3 MV tandetron accelerator at the ion beam facility in Rossendorf [13]. The ion beam was electrostatically scanned across a 5.1×5.1 cm^2 area. The ion energy was varied between 2 and 16 MeV and fluences ranged from 2×10^{14} to 11×10^{14} cm^{-2}. The ion beam energy flux was kept constant at a value of 0.16 W/cm^2 during all irradiations. The substrate holder was cooled to 77 K with liquid nitrogen and all irradiations were performed at an angle of 45° with respect to the Si surface. Vacuum grease at the backside of the sample was used to improve the heat contact between the sample and the cooled substrate holder. Ion ranges and electronic energy losses were calculated using TRIM98 [14], a Monte Carlo calculation, using a silica structure with a density of 2.0 g/cm^3 [15].

ZnS and ZnS/SiO_2 core/shell particles as well as micro-crystalline Ag particles were synthesized using methods described in [16–18]. TiO_2 colloids were made as described in [19], and single-crystalline α-Al_2O_3 particles were obtained from Sumitomo Chemical (Japan). All these particles were irradiated with a 4 MeV Xe ion beam at 77 K. The ion beam was electrostatically scanned across a 2.7×2.7 cm^2 area at a flux of ~ 0.02 W/cm^2.

Scanning electron microscopy (SEM) was performed at an energy of 10 keV under different angles to image the particle shape before and after irradiation. Image processing and analysis software was used to characterize the particles before and after irradiation.

3. Results and discussion

3.1. Silica colloids

Fig. 1(a) shows a SEM image of unirradiated silica particles on a silicon substrate viewed under normal incidence (see schematic in Fig. 1). The size distribution of 65 analyzed colloids is displayed in Fig. 2 (black histogram). The average colloid diameter was 1004 ± 20 nm [1] with a standard deviation characterizing the size polydispersity $\sigma = 31$ nm. This is typical for the colloid fabrication method used [12].

Next, the colloids were irradiated with a 14 MeV Au ion beam to a fluence of 4×10^{14} cm^{-2}, under an angle of 45° (see schematic in Fig. 1). The projected ion range was calculated to be about 3.5 μm, well beyond the particle diameter. Fig 1(b) shows a SEM micrograph after irradiation taken in the direction perpendicular to the ion beam. Clearly, the originally spherical particle has turned into an ellipsoidal oblate with a dimensional

[1] The error includes the error in the average determined from the size histogram and the pixel dimension in the SEM images.

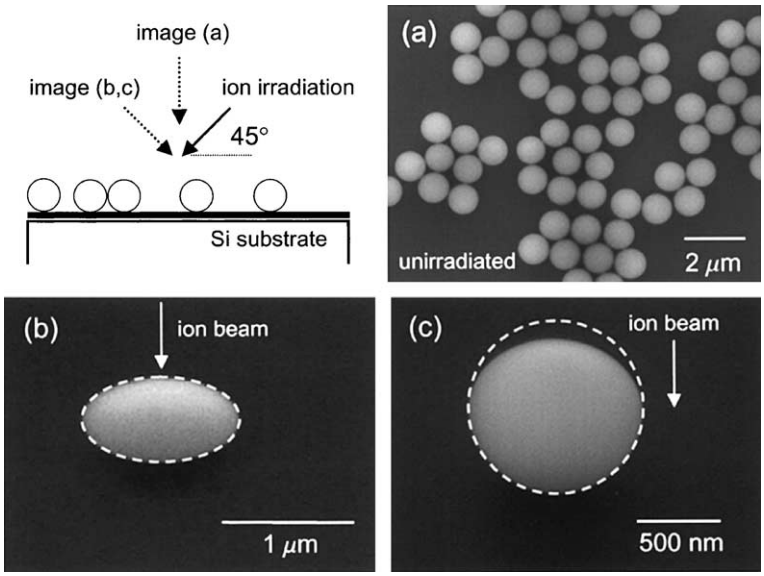

Fig. 1. SEM images of unirradiated and Au ion irradiated silica colloids on a silicon substrate. The ion beam direction and the different SEM viewing angles are depicted in the schematic. The arrows in the SEM images indicate the direction of the ion beam. (a) Unirradiated silica colloids in top view. (b) Deformed silica colloid after irradiation with 14 MeV Au ions to a dose of 4×10^{14} cm^{-2} under 45° at 77 K. (c) Deformed silica colloid after a similar irradiation with 2 MeV Au ions. Circular and ellipsoidal shapes are shown for reference by the dashed lines.

expansion perpendicular to the ion beam and a contraction parallel to the ion beam.

Fig. 2 also shows the size distribution of the transverse diameter of 33 oblates after irradiation (gray histogram). This axis has increased to a mean value of 1181 ± 20 nm, with $\sigma = 27$ nm. This indicates that the ion irradiation process does not significantly increase the particle size polydispersity. Note that at a fluence of 4×10^{14} cm^{-2} each colloid has been impacted by some 10^7 ions. Any statistical variations are expected to be averaged out at this large number of ions. Assuming the colloidal volume remains constant after irradiation [10], the aspect ratio (ratio of transverse and longitudinal diameter) of the deformed colloids in Fig. 1(b) is calculated to be 1.63.

Fig. 1(c) shows a SEM micrograph of a colloid after irradiation with 2 MeV Au ions to a fluence of 4×10^{14} cm^{-2} viewed in the direction perpendicular to the ion beam. The projected range of 2 MeV Au ions in SiO_2 is about 0.55 μm, roughly equal to half the colloid diameter. This implies that the lower half of the colloid is not fully irradiated, except at the lateral side edges. Fig. 1(c) clearly shows a non-ellipsoidal shape of the colloid: the upper part of the colloid is deformed whereas the lower part remains undeformed (see white dashed line). This clearly indicates that the deformation only takes place in the irradiated region of the colloid. From this, we can conclude that the plastic deformation does not result from a uniaxial hydrostatic pressure generated by the ion beam, but results from single ion impacts only. This is in agreement with the thermal spike model.

To investigate the energy dependence of the deformation, silica spheres were irradiated with Au ions at energies ranging from 4 to 16 MeV to a fixed fluence of 4×10^{14} cm^{-2}. Fig. 3 shows the measured relative change of the transverse diameter after irradiation, plotted as a function of the electronic stopping power in the colloid. The latter is calculated using a three-dimensional averaging method taking into account the changing shape of the colloid during irradiation. Also included in Fig. 3 is a data point obtained for 500 keV Xe irradiation of 290 nm silica colloids at a fluence of

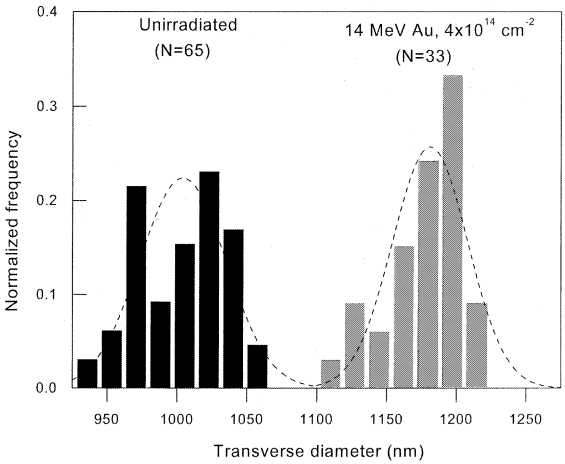

Fig. 2. Histogram of the transverse diameter size distribution of unirradiated silica colloids (black bars) and silica colloids irradiated with 14 MeV Au ions to a fluence of 4×10^{14} cm^{-2} (gray bars). Gaussian distributions with standard deviations of $\sigma = 31$ nm (unirradiated) and $\sigma = 27$ nm (irradiated) are indicated by the dashed lines.

1×10^{16} cm^{-2}, for which no deformation is found (solid square).

Fig. 3 shows that the transverse diameter increases with average electronic energy loss.

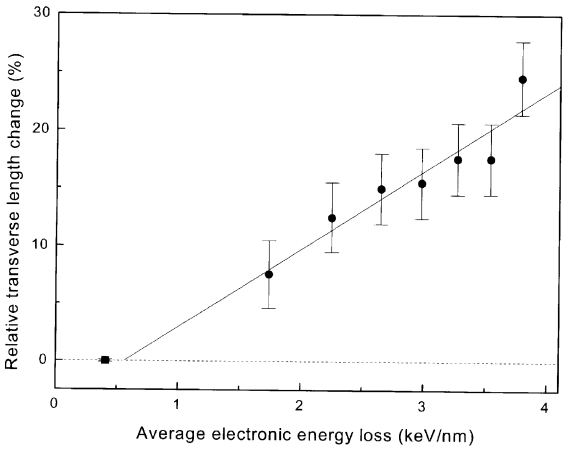

Fig. 3. Relative change of the transverse diameter of the silica oblates as a function of the average electronic energy loss at a fixed fluence of 4×10^{14} cm^{-2}. Data were taken from experiments using ion energies in the range 4–16 MeV Au. The drawn line is a linear fit to the data. A data point for 500 keV Xe irradiation (1×10^{16} cm^{-2}) of 290 nm colloids for which no deformation was found is also indicated (solid square).

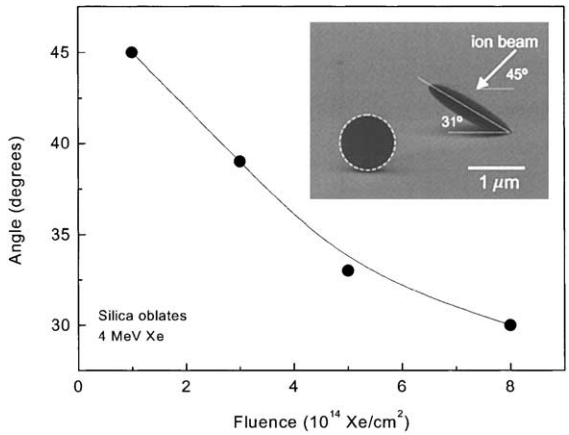

Fig. 4. Angle between substrate and transverse axis of deformed silica colloids, as observed in side-view SEM images (15° tilt), as a function of ion fluence. Irradiations were performed using a 4 MeV Xe ion beam at 77 K. The drawn curve is a guide to the eye. The inset shows a side-view SEM image (8° tilt) of a silica colloid irradiated with a 16 MeV Au ion beam to a dose of 11×10^{14} cm^{-2} at 77 K.

Because no deformation has been observed at a low energy, there is an apparent threshold below which no deformation occurs. This threshold value is at least 0.41 keV/nm (500 keV Xe irradiation data point) and is interpolated to have value of ~0.6 keV/nm (using Au irradiation data). A threshold has also been found for the irradiation of silica foils, though larger in magnitude (2 keV/nm) [2]. The apparent threshold can be explained in terms of a transition from a more or less isotropically shaped collision cascade for low energy irradiation, for which no anisotropic deformation occurs, to an anisotropically shaped thermal spike along the ion track at high energy [2].

Fig. 4 (inset) shows a side-view SEM image of a silica particle with the highest size-aspect ratio obtained so far (4.7). A 16 MeV ion beam, incident at 45°, was used at a fluence of 11×10^{14} cm^{-2}. An unirradiated spherical colloid is also observed and must have jumped over from the unirradiated part of the sample after the irradiation. At this large deformation it is observed that the angle between the long particle axis and the substrate is only 31°. To obtain more insight in this effect, measurements of the particle angle were performed as a function of

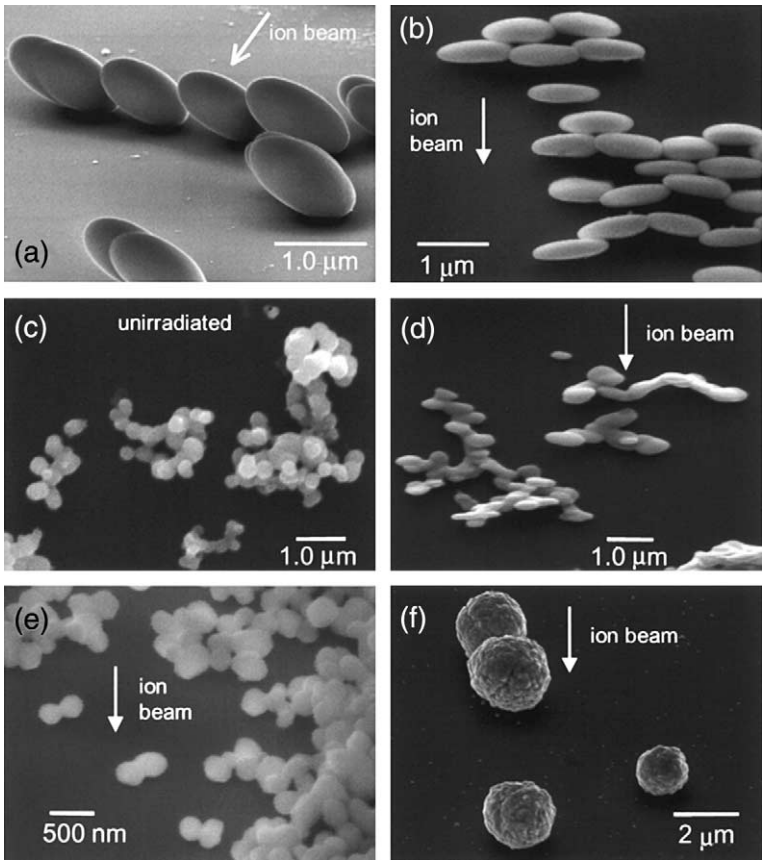

Fig. 5. SEM images of ion irradiated colloids of various materials. The irradiations were all performed using a 4 MeV Xe ion beam at 77 K. The direction of the ion beam is indicated by the arrows. All images were taken as in projection (b) in the schematic of Fig. 1 (except (a), that was taken from the side at a 15° tilt): (a) irradiated micro-crystalline ZnS (5×10^{14} cm^{-2}), (b) irradiated ZnS/SiO_2 core/shell particles (4×10^{14} cm^{-2}), (c) unirradiated amorphous TiO_2, (d) irradiated amorphous TiO_2 (3×10^{14} cm^{-2}), (e) irradiated single-crystalline Al_2O_3 (4×10^{14} cm^{-2}), and (f) irradiated micro-crystalline Ag (4×10^{14} cm^{-2}).

ion fluence (Fig. 4). [2] A 4 MeV Xe ion beam was used at fluences ranging from 1×10^{14} to 8×10^{14} cm^{-2}. An angle of 45° is observed for small fluences (1×10^{14} cm^{-2}), while for higher fluences a gradual decrease is observed. From the known sample geometry during irradiation we can exclude gravity as a cause of the effect. Two possible explanations of the particle tilt come to mind: (1) momentum transfer [20] from the incident ions to the particle which then rotates around its contact point with the substrate; (2) a gradual change in the geometry of the contact area between the colloid and the substrate due to the particle expansion. Because no difference in contact angle is observed for small (290 nm diameter) and large ($\sim$ 1 μm diameter) irradiated silica colloids, a geometric effect seems to be more likely than a ballistic effect.

3.2. Other materials

Fig. 5 shows SEM images of colloidal particles of several other materials, all irradiated with 4 MeV Xe ions. A side view image of micro-crystalline ZnS particles irradiated at a fluence of

[2] As no data are yet available for the dependence of angle on fluence for Au irradiation, we present data for Xe irradiation.

5×10^{14} cm^{-2} is shown in Fig. 5(a). The size-aspect ratio of these particles is 2.2. This is similar to what is observed for silica particles irradiated under the same conditions [10]. Fig. 5(b) shows deformed core/shell particles composed of a 692 nm diameter ZnS core covered by a 5 nm thick SiO_2 shell after irradiation with 4×10^{14} Xe cm^{-2}. The observed size-aspect ratio is about twice as large as what would be observed for the individual materials at this same fluence. At present this difference remains to be explained.

Next, we studied the deformation of amorphous TiO_2 colloids. These particles cannot be made with the small size polydispersity as is common for the SiO_2 and ZnS colloids, as can be seen in Fig. 5(c). However a deformation after irradiation (3×10^{14} Xe cm^{-2}) can clearly be seen in Fig. 5(d). This demonstrates the versatility of the ion irradiation technique to deform a wide variety of materials.

Fig. 5(e) shows single-crystalline Al_2O_3 colloids after irradiation with 4×10^{14} Xe cm^{-2}. Although less easy to identify in the SEM image because of the particle clustering, we find no evidence for anisotropic deformation of this material. Similarly, micro-crystalline Ag colloids (4×10^{14} Xe cm^{-2}, Fig. 5(f)) show no deformation. The fact that no deformation is observed in crystalline materials is consistent with earlier work on the deformation of thin foils [21]. Within the thermal spike model of deformation, a crystalline material would not deform because of the large resistance (high viscosity, no free volume) to deformation. In addition, for metals the molten region in the spike would recrystallize so rapidly that it may not lead to deformation.

Finally, we note that the deformation of micro-crystalline ZnS colloids (Fig. 5(a)) may seem inconsistent with the argument that crystalline materials do not deform. However, these particles may have amorphized under irradiation. This feature is presently under investigation.

4. Conclusions

Spherical colloidal silica particles undergo anisotropic plastic deformation under 2–16 MeV Au irradiation. The size polydispersity is not affected by the ion beam. The transverse diameter increases with the average electronic energy loss in the colloid, above a threshold value of ~ 0.6 keV/nm. Non-ellipsoidal shapes are formed when the ion range is smaller than the colloid diameter. Anisotropic plastic deformation was also observed for micro-crystalline ZnS, ZnS/SiO_2 core/shell and amorphous TiO_2 particles. No deformation was found for single-crystalline Al_2O_3 and micro-crystalline Ag particles. All data are consistent with the thermal spike model of deformation.

Acknowledgements

We gratefully acknowledge W.A.M. van Maurik (Utrecht University) for his support with the electron microscopy, G.E. Zegers for making the Ag particles (Utrecht University, unpublished work), and M.P. van Bruggen (Philips Research) for providing Al_2O_3 colloids. This work is part of the research program of the Foundation for Fundamental Research on Matter (FOM) and was financially supported by the Dutch Organization for Scientific Research (NWO). It was also supported by the EC Large Scale Facility "AIM-Center for Application of Ion Beams in Materials Research", project no. ERB FMGE CT98 0146.

References

[1] M-d. Hou, S. Klaumünzer, G. Schumacher, Phys. Rev. B 41 (1990) 1144.
[2] A. Benyagoub, S. Löffler, M. Rammensee, S. Klaumünzer, G. Saemann-Ischenko, Nucl. Instr. and Meth. B 65 (1992) 228.
[3] S. Klaumünzer, A. Benyagoub, Phys. Rev. B 43 (1991) 7502.
[4] E. Snoeks, A. Polman, C.A. Volkert, Appl. Phys. Lett. 65 (1994) 2487.
[5] M.L. Brongersma, E. Snoeks, T. van Dillen, A. Polman, J. Appl. Phys. 88 (2000) 59.
[6] H. Trinkaus, A.I. Ryazanov, Phys. Rev. Lett. 74 (1995) 5072.
[7] H. Trinkaus, Nucl. Instr. and Meth. B 146 (1998) 204.
[8] A.I. Ryazanov, A.E. Volkov, S. Klaumünzer, Phys. Rev. B 51 (1995) 12107.
[9] E. Snoeks, T. Weber, A. Cacciato, A. Polman, J. Appl. Phys. 78 (1995) 4723.

[10] E. Snoeks, A. van Blaaderen, T. van Dillen, C.M. van Kats, M.L. Brongersma, A. Polman, Adv. Mat. 12 (2000) 1511.
[11] E. Snoeks, A. van Blaaderen, T. van Dillen, C.M. van Kats, K. Velikov, M.L. Brongersma, A. Polman, Nucl. Instr. and Meth. B 179 (2001) in press.
[12] A. van Blaaderen, A. Vrij, Langmuir 8 (1993) 2921.
[13] M. Friedrich, W. Bürger, D. Henke, S. Turuc, Nucl. Instr. and Meth. A 382 (1996) 357.
[14] J.F. Ziegler, J.P. Biersack, U. Littmark, in: The Stopping and Range of Ions in Solids, Pergamon, New York, 1985.
[15] A. van Blaaderen, A.P.M. Kentgens, J. Non-Cryst. Solids 149 (1992) 161.
[16] S.M. Scholz, R. Vacassy, J. Dutta, H. Hofmann, M. Akinc, J. Appl. Phys. 83 (1998) 7860.
[17] S.M. Scholz, R. Vacassy, L. Lemaire, J. Dutta, H. Hofmann, Appl. Organometal. Chem. 12 (1998) 327.
[18] K.P. Velikov, A. van Blaaderen, submitted to Langmuir; preliminary results were published, in: A. van Blaaderen, MRS Bulletin 23 (1998) 39.
[19] J.H. Jean, T.A. Ring, Langmuir 2 (1986) 251.
[20] L. Cliche, S. Roorda, M. Chicoine, R.A. Masut, Phys. Rev. Lett. 75 (1995) 2348.
[21] A. Benyagoub, S. Klaumünzer, L. Thomé, J.C. Dran, F. Garrido, A. Dunlop, Nucl. Instr. and Meth. B 64 (1992) 684.